# A PERSPECTIVE ON EPOXY/GRAPHITE-BASED COMPOSITES FOR ELECTROMAGNETIC INTERFERENCE SHIELDING: FABRICATION AND APPLICATION IN SECURITY TECHNOLOGIES

**Stevan Stupar**[1], **PhD**
**Nemanja Vučković, PhD**
**Nikola Milašinović, PhD**
University of Criminal Investigation and Police Studies, Belgrade, Serbia

**Mladen Timotijević, MSc**
Ministry of Defence, Military Technical Institute, Belgrade, Serbia

## ABSTRACT

**Purpose:** The rapid advancement of technology brings numerous benefits, such as facilitating everyday processes in households, laboratories, and production environments. However, many modern electronic devices used in forensic laboratories and police units require electromagnetic compatibility for efficient operation. To overcome this challenge, an effective solution is the design of protective covers made from lightweight, high-efficiency composite materials.

**Design/Methods/Approach:** This study presents a method for modifying the surface of graphite particles by silver deposition and their implementation in epoxy-based composite materials. Graphite particles were treated with the prepared silver dispersion, while FESEM/EDS, XRF, and electrical conductivity analyses were conducted to assess the properties of the modified particles. The polymer characteristics were evaluated through viscosity determination and dynamic mechanical thermal analysis. The study examined how the mechanical properties of composites relate to the mass fraction of modified graphite particles and the effectiveness of electromagnetic interference shielding (EMI SE) in the X-band.

**Findings:** Analysis of the modified graphite particles revealed a significant concentration of elemental silver on graphite surfaces to improve electrical conductivity. Increasing the conductivity of particles contributes to the formation of a Faraday cage, which can find application in increasing the electromagnetic compatibility of electronic devices. The incorporation of the silver coating onto graphite particles' surface improved the physical and mechanical properties of the particles and composites. The average wave intensity attenuation increased by 21% with silver coating compared to samples without it.

**Originality/Value:** This paper presents a cost-effective method for modifying the surface of graphite particles via silver deposition following dispersion evaporation. A key advantage of this method is that it does not require expensive equipment or high energy consumption and also does not generate large amounts of waste that would need special treatment. Moreover, the study explores the potential practical application of the composites for preventing electromagnetic interference in security technologies.

**Keywords:** electromagnetic interference shielding, graphite, silver deposition, functional materials, surface conductivity.

1 stevan.stupar@kpu.edu.rs

## *About the authors*

**Stevan Stupar**, Ph.D., graduated from the Department of Military Chemical Engineering at the Military Academy and completed both his master's and doctoral studies at the Faculty of Technology and Metallurgy at the University of Belgrade. Since 2021, he has held the title of Ph.D. in Technological Engineering. He is currently an assistant professor at the Faculty of Forensic Sciences and Engineering, at the University of Criminal Investigation and Police Studies. His research focuses on the synthesis and characterization of functional materials for various applications. A significant aspect of his work involves developing composite materials designed to prevent electromagnetic interference using electrically conductive and ferromagnetic particles. Stevan Stupar has co-authored 16 scientific papers published in peer-reviewed journals.

**Mladen Timotijević**, M.Sc., graduated from the Military Academy in 2017 and earned his master's degree from the same institution in 2022. Upon graduation, he served in the Serbian Armed Forces until 2022, after which he joined the Military Technical Institute, where he is currently employed in the Sector for Materials and Protection, Department for Energetic Materials. During the academic year 2020/2021, he worked as a teaching associate at the Military Academy. He is currently pursuing his doctoral studies at the Faculty of Technology and Metallurgy, University of Belgrade. His research interests include composites and polymers applied in materials, with a focus on their development, characterization, and application in defense technologies.

**Nemanja Vučković**, Ph.D., earned his doctorate degree in Technology Engineering in 2025 from the University of Criminal Investigation and Police Studies, at the Faculty of Forensic Sciences and Engineering, where he currently works as an assistant professor. Since 2014 he has been actively engaged as a demonstrator at educational events/fairs, where he demonstrated the capabilities of routinely used methods, as well as novel approaches for developing latent fingerprints. Since 2016 he has been an active member of the Forensic Polymer Section, where he conducts research on synthesis, characterization, and application of various types of polymers in the field of forensic trace analysis, but also in different fields of technology engineering.

**Nikola Milašinović**, Ph.D., is a Chemical and Material Science Engineer that earned his doctorate degree in 2011 from the Faculty of Technology and Metallurgy, University of Belgrade. He has been working on several long-term projects covering the syntheses of different types of polymer matrices/devices suitable for encapsulation/immobilization of various active substances. Since October 2016 he has held the position of Head of the Forensic Polymer Section. His research covers the synthesis and characterization of various natural/synthetic polymer-conjugated systems that could be applied in police everyday practice.

## INTRODUCTION

The rapid development of electronic devices in all sectors of the modern life cycle has led to a significant increase in electromagnetic interference (EMI) between electronic devices. This problem poses significant threats to the performance, reliability, and safety of sensitive electronic systems, potentially causing operational disruptions, data corruption, and even unintentional signal interception (Yan & Cao, 2021; Zheng et al., 2022). In critical areas such as security technologies, the negative effects of EMI can have serious consequences, requiring robust and effective EMI SE solutions (Greety & Wessley, 2024). In the field of security technologies, and especially for police services, the reliable operation of electronic equipment is undeniable. Electromagnetic compatibility plays a key role in protecting critical operational capabilities:

- Ensuring communication integrity: Police operations rely heavily on secure and uninterrupted communication systems (e.g., radios, tactical communications devices). EMI SE materials usually focus on shielding sensitive transceivers and antennas from external noise, preventing communication disruptions and ensuring clear, reliable command and control during critical incidents (Hamamah et al., 2019).
- Protecting surveillance and sensor systems: Electronic tools such as body-worn cameras, vehicle-mounted surveillance systems, radar guns, and biometric scanners are fundamental to modern policing. Electromagnetic interference shielding materials (SE) shield these devices from interference, ensuring accurate data recording and reliable operation, which is vital for evidence collection and tactical decision-making (Wiśnios et al., 2025).
- Maintaining the reliability of vehicle electronics: Modern police vehicles are sophisticated platforms equipped with a multitude of electronic systems, from engine management to vehicle computing and navigation. Shielding ensures that these critical systems operate flawlessly, preventing electromagnetic "noise" from the vehicle or external sources from causing malfunctions that could compromise officer safety or mission success (Hu et al., 2019).
- Data and Information Security: In an era of increasing digital dependency, protecting sensitive data stored and transmitted by police equipment is of paramount importance. EMI shielding contributes to information security by reducing the risk of electronic eavesdropping or data corruption caused by electromagnetic radiation, thereby maintaining the integrity of intelligence and evidence (Yu-ichi Hayashi, 2016).

Traditional approaches to electromagnetic shielding, which often involve metal enclosures, often present limitations in terms of weight, corrosion susceptibility, and adaptability to complex system designs (Hong et al., 2024). This has prompted intensive research into advanced materials capable of offering lightweight, flexible, and highly efficient electromagnetic shielding. The attenuation of electromagnetic waves can be achieved through the development of advanced materials that integrate both absorptive and reflective mechanisms across multiple layers (Gahlout & Choudhary, 2019). The shielding performance of such materials is conventionally expressed as the cumulative contribution of absorption, reflection, and a correction factor that accounts for multiple internal reflections within the shielding medium (Serhan et al., 2019). For a material to be regarded as highly effective in electromagnetic wave mitigation, it must possess appropriate dielectric properties, sufficient magnetic permeability, adequate thickness, and stable performance across the relevant frequency ranges (Fu et al., 2022; Hwan et al., 2019). On the basis of these criteria, shielding materials are generally classified into several groups, including metallic systems (Stupar et al., 2023), carbon-based allotropes and derivatives (Cheng et al., 2023; Stupar et al., 2022), electrically conductive polymers (Uma Varun et al., 2019), and ferromagnetic compounds (Iqbal et al., 2019). Furthermore, hybrid materials can be synthesized through the combination of multiple constituents in order to integrate complementary properties required for efficient EMI SE (Bhardwaj & Nirmala, 2020; Uma Varun et al., 2019). Depending on their composition and intended application, these materials may be fabricated as metallic frameworks, polymer matrix composites, or functional coatings for textile substrates (Stupar et al., 2022; Y. Z. Zhang et al., 2020). A variety of surface modification techniques have been reported in the literature, including in-situ polymerization (Greety & Wessley, 2024), sputtering (Wang et al., 2020), layer-by-layer assembly (Wang et al., 2020), ionotropic gelation and conjugation (Vučković et al., 2021), and spin-coating (J. Zhang et al., 2022).

Among the most promising candidates are polymer matrix composites, especially those based on epoxy resins reinforced with conductive fillers such as electric conductive materials like graphite (Stupar et al., 2025). Carbon-based materials are widely utilized as reinforcement agents in aerospace, automotive, and defence applications owing to their mechanical robustness, durability, and ease of processing (Behera et al., 2024; J. Zhang et al., 2022). Their outstanding mechanical performance, coupled with high electrical and thermal conductivity, enhances composite functionality and contributes to improved EMI SE (J. Zhang et al., 2022). This study provides a comprehensive perspective on epoxy/graphite composites for EMI protection. Also, examine various fabrication techniques for integrating graphite into epoxy matrices, discuss the underlying mechanisms of EMI shielding, and evaluate their performance characteristics. In addition, this study addresses the specific applications and benefits of these advanced composites within security technologies, highlighting their essential role in improving the operational resilience and security posture of police services against electromagnetic threats. These epoxy/graphite composites offer a unique combination of mechanical strength, processability, and tunable electromagnetic properties, making them ideal for next-generation shielding applications. Although conventional techniques for depositing metal nanoparticles onto conductive and non-conductive particle surfaces are effective, they often demand elevated temperatures and rely on hazardous and costly reagents. In contrast, dispersion evaporation (Liu & Xu, 2020) has emerged as a promising alternative for surface modification and nanocomposite fabrication. This technique of particles` modification employs inexpensive, non-toxic reagents and operates without the necessity for high-temperature conditions or significant electrical input.

Therefore, the objective of this study is to develop and evaluate silver-modified graphite/epoxy composites prepared via dispersion evaporation, with the aim of enhancing EMI SE of graphite particles while maintaining cost efficiency, material processability, and characterization. This study represents the first systematic study of general usage of graphite (unmodified and modified) particles for EMI SE, along with our previous study (Stupar et al., 2025).

## EXPERIMENTAL PART

### *Silver conductive dispersion synthesis – reagents and materials*

The synthesis of the silver conductive solution was performed by the modified Tollens process, which was described in detail by Stupar et al. (Stupar et al., 2023). First, 15 g of silver acetate ($CH_3COOAg$, 99.0 %, Sigma-Aldrich (USA)) was dissolved in 37.5 ml of ammonium hydroxide solution ($NH_4OH$, 30%, Zorka Pharma-Hemija (Serbia)) at room temperature. After 20 minutes, 1 ml of formic acid (HCOOH, 98.0%, Sigma-Aldrich (USA)) was added to the solution. The mixture was then stirred for 24 hours and filtered using a 0.45 nm nylon syringe filter (Sartorius, Germany).

### *The Graphite Particles' Surface Modification by Dispersion Evaporation and Composite Preparation*

Graphite powder (100 g, Acros Organics, USA) was functionalized by immersion in silver conductive dispersion at three distinct volumes: 50, 100, and 150 ml. This variation yielded samples with different graphite-to-electrically conductive dispersion ratios, subsequently designated as 0.5, 1.0, and 1.5 Graphite@Ag particles, respectively, reflecting the ratio of solid to liquid phases. Each mixture was subjected to thorough mixing in a dark environment at ambient temperature for a period of 24 hours. Initial drying was conducted by air exposure at room temperature to facilitate the evaporation of ammonia from the dispersion. This process was evidenced by a notable color transition from black to silver and the liberation of a distinct formic acid odor. Following ambient evaporation, the powder samples underwent thermal treatment at 80° C for 60 minutes within a thermostatic chamber (G209A, SDL Atlas, UK), accompanied by intermittent stirring with a glass rod. This heating step is critical for the complete volatilization of formic acid from the silver conductive dispersion and the robust formation of an elemental silver film on the graphite particle surfaces. After heat treatment, the samples were washed using methyl alcohol ($CH_3OH$, 99.8%, Merck Group (Germany)) and dried at room temperature.

The synthesized silver-coated graphite powders, along with a commercial graphite powder for comparative analysis, were homogeneously dispersed in an epoxy resin matrix (Type W300, R&G Faserverbundwerkstoffe GmbH, Germany). The filler loading was systematically varied across a range of 10 to 40 weight percent (wt.%). The prepared composite mixtures were then cast into appropriate molds to facilitate subsequent physical, mechanical, and EMI SE characterizations. Following mixing, the composites were cured by drying in a vacuum chamber (VD 23, Binder, Germany) at 80° C for 24 hours.

### *Characterization and Measurement*

The microstructure and morphology of unmodified and modified particles and semi-quantitative elemental analyses were studied by field-emission scanning electron microscopy with Energy-Dispersive X-ray Spectroscopy (JEOL JSM 7001F, Japan). The Graphite@Ag powder samples were evaluated by a Vanta Max series portable handheld X-ray fluorescence (XRF) spectrometer (Olympus, Germany). The XRF spectrometer had a rhodium source, an SSD detector, 4 W maximum power output, 50 kV, and eight filters. Measurement conditions were 40 kV, 1 mA for 30 s under air. Particle size distributions of the Graphite@Ag suspensions were determined by laser diffraction in wet mode using an Anton Paar PSA 1190. Deionized water served as the dispersant, and Igepal CA-630 was added to enhance particle wetting. The slurry was homogenized by stirring for 5 min. with ultrasonication at 50 W. Data were evaluated with Mie theory assuming a refractive index of 2.0 and an absorption (imaginary) index of 1.0. Steady-shear viscosity was measured on an Anton Paar MCR 302 rheometer equipped with a concentric-cylinder CC27 geometry, in accordance with ISO 3219, at 25.0 ± 0.1°C. The shear rate was stepped logarithmically from 0.1 to 1000 $s^{-1}$ (10 equidistant logarithmic points per decade), while the dwell time per point decreased from 30 s to 1 s on a logarithmic schedule. Torsional DMTA was performed on rectangular specimens using the same rheometer fitted with a CTD-620 temperature chamber and SRF12 fixtures. Samples had approximate dimensions of 3 mm × 10 mm × 54 mm. Temperature sweeps from 0 to 80 °C were conducted at 2°C·$min^{-1}$ with a constant frequency of 1 Hz and a constant logarithmic strain amplitude of 0.1% (within each material's linear viscoelastic range).

The dielectric parameters of a material are measured by the waveguide method, where the cross section of a rectangular waveguide determines the frequency range to be evaluated. In this experiment, according to the X-band waveguide dimensions, the material was processed into a size of 22.8 mm × 10.15 mm × 2.0 mm. The samples were sanded and polished, then cleaned and dried, and the dielectric parameters were tested using a vector network analyzer (Agilent, model number PNA-N5244A). The electrical resistivity of particles was determined by 4-wire measurements using RM3000+ (Jandel, UK). Samples for testing electrical conductivity were made by pressing pellets with a thickness of 1 mm. The applied pressure per pressing tool is 200 bar, and the hydraulic press type HZVT 2.5 (Dunkes, Germany) was used.

## RESULTS AND DISCUSSION

### *SEM/EDS Analysis*

Structural, morphological, and semi-quantitative characterizations of Graphite@Ag particles and their composites were conducted using scanning electron microscopy (SEM) coupled with energy-dispersive X-ray spectroscopy (EDS). SEM photographs shows Graphite@Ag particles prepared with varying amounts of silver conductive dispersion, as well as the corresponding Graphite@Ag/epoxy composites, are displayed in Figure 1. Figure 2 presents both the SEM images and EDS spectra for Graphite@Ag(1.0) particles and the epoxy resin containing 30 wt.% Graphite@Ag(1.0) particles.

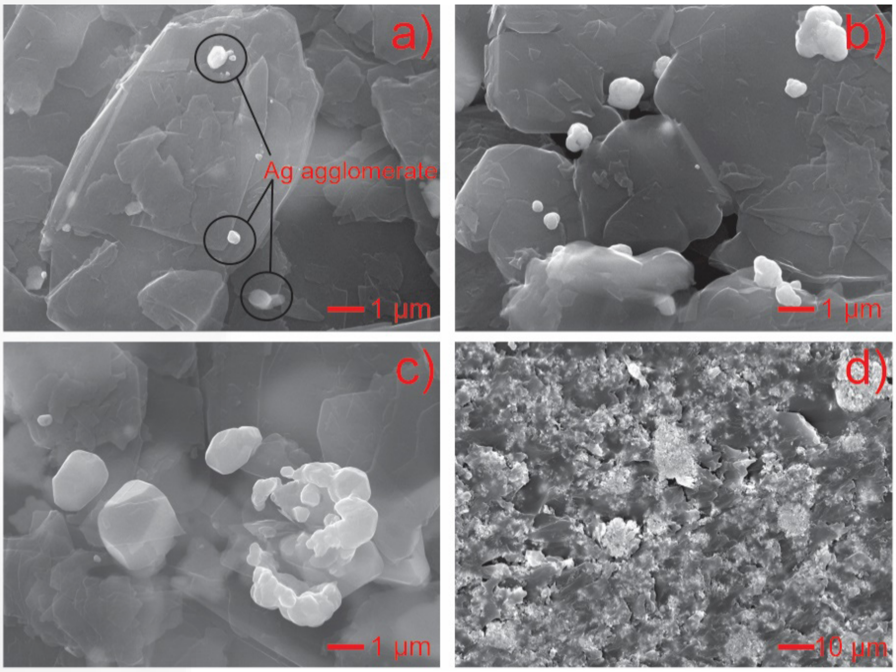


**Figure 1:** *The SEM micrographs of 0.5 a), 1.0 b), and 1.5 c) Graphite@Ag particles and 30 wt.% Graphite@Ag particles (1.0)/epoxy composite d).*

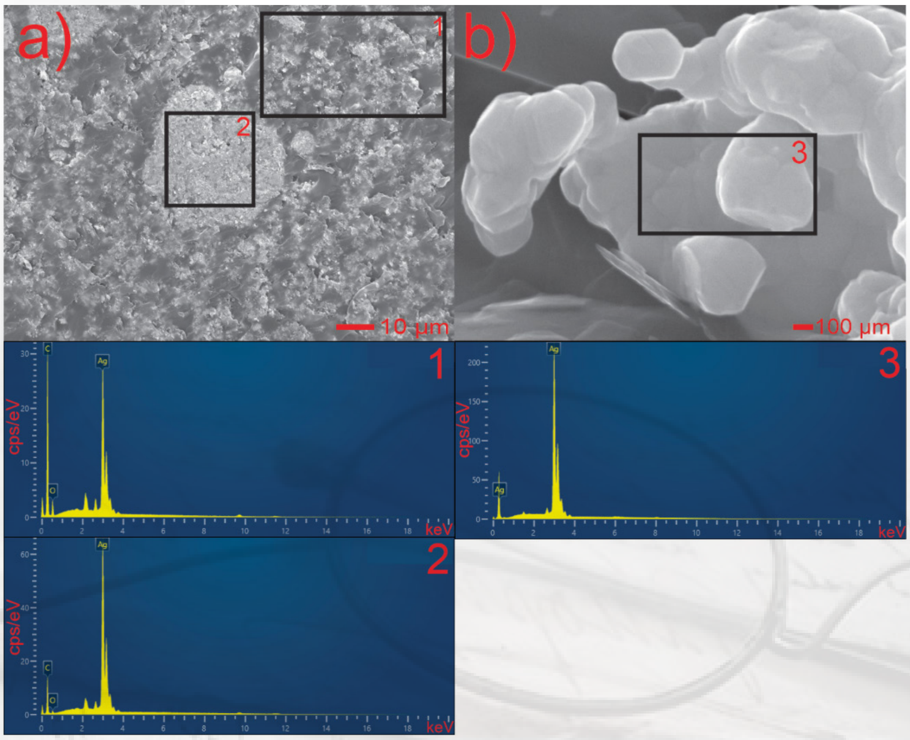


**Figure 2:** *The SEM micrograph and EDS spectra of 30%Graphite@Ag(1.0)/epoxy a) and silver particles agglomerate deposited onto graphite particle b).*

Micrographs presented in Figure 1 indicate that the appearance of silver agglomerates is significantly influenced by the amount of electroconductive dispersion used. In the case of the Graphite@Ag particles with 0.5 dispersion, agglomerates are minimal, whereas with the Graphite@Ag particles using 1.5 dispersion, a higher concentration of silver nanoparticle agglomerates is observed on the surface of the graphite particles. This finding aligns with the research conducted by Stupar et al. (Stupar et al., 2022), where scanning electron microscopy was utilized to examine carbon fabrics modified with silver particles. Their study confirmed that the number of agglomerates on the fabric's surface increases with repeated soaking in a silver complex dispersion.

Figure 2 highlights the excellent coverage of the epoxy matrix with Graphite@Ag particles. Additionally, the energy-dispersive spectroscopy (EDS) analysis of composite area 1 reveals the presence of carbon, silver, and oxygen, comprising 54.34%, 34.62%, and 11.05% by weight, respectively. In the second EDS spectrum (area 2), the corresponding values are 23.32%, 4.25%, and 72.43% by weight. Figure 2b illustrates a pure agglomerate of silver particles.

## *XRF Analysis*

According to the XRF analysis, the amount of silver in Graphite@Ag (0.5), (1.0), and (1.5) particles and the Graphite@Ag (1.0)/epoxy resin composite was 9.93, 20.59, 26.51, and 33.85 wt.%, respectively. The XRF analysis confirms the dependence of silver deposition on the amount of the silver conductive dispersion. The XRF spectra of pure graphite (a), Graphite@Ag(0.5) (b), Graphite@Ag(1.0) (c), Graphite@Ag(1.5) (d), and 30%Graphite@Ag(1.0)/epoxy composite are shown in Figure 3. Peak characteristics of elemental silver are marked on all XRF spectra shown in Figure 3.

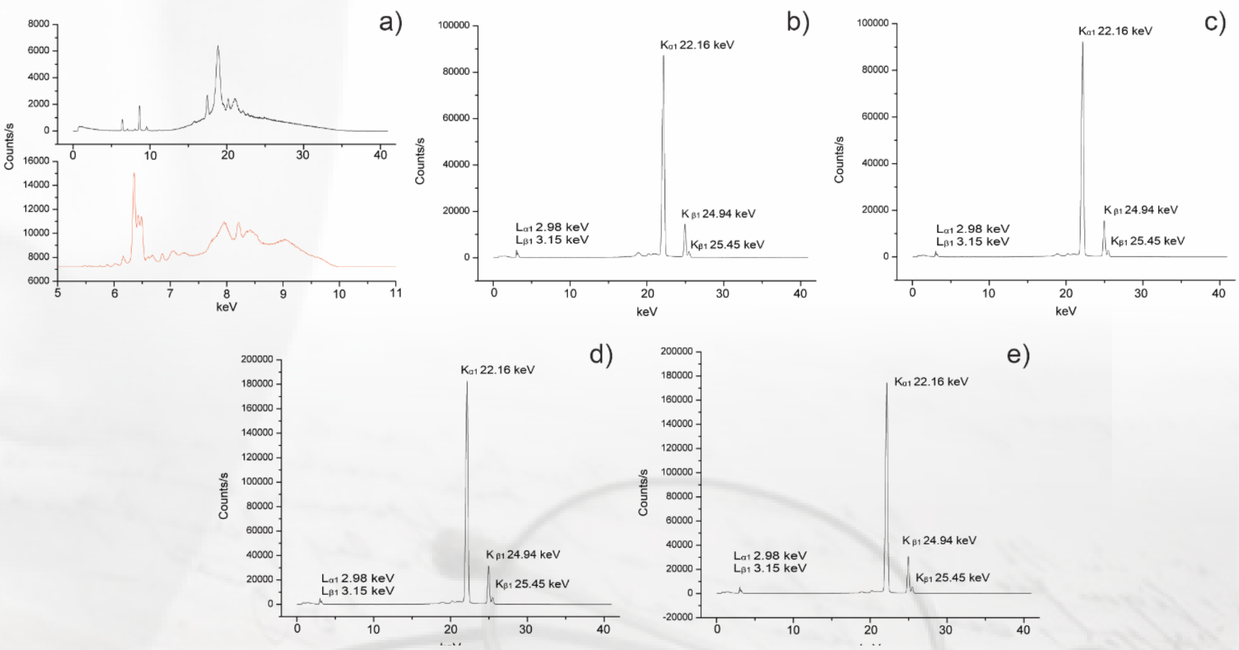


**Figure 3:** *The XRF spectra of pure graphite (a), Graphite@Ag(0.5) (b), Graphite@Ag(1.0) (c), Graphite@Ag(1.5) (d), and 30%Graphite@Ag(1.0)/epoxy composite (e).*

## *Rheological Properties*

The systematic quantification of the relationship between composition and rheology provides a rigorous foundation for defining processing windows and application conditions. Steady-shear measurements were used to determine the apparent viscosity as a function of shear rate, η(γ̇) (Figure 4a), and the corresponding flow curves, τ(γ̇) (Figure 4b), for uncured epoxy suspensions containing varying mass fractions of Graphite@Ag(1.0). In addition, oscillatory tests provided application-relevant rates of different wt.% of Graphite@Ag(1.0) particles in the suspension viscoelastic parameters: the storage modulus G′ (Figure 5a) and the loss modulus G″ (Figure 5b). For completeness, the composition-dependence of G″ is summarized in Figure 6a, while the particle-size distribution is presented in Figure 6b.

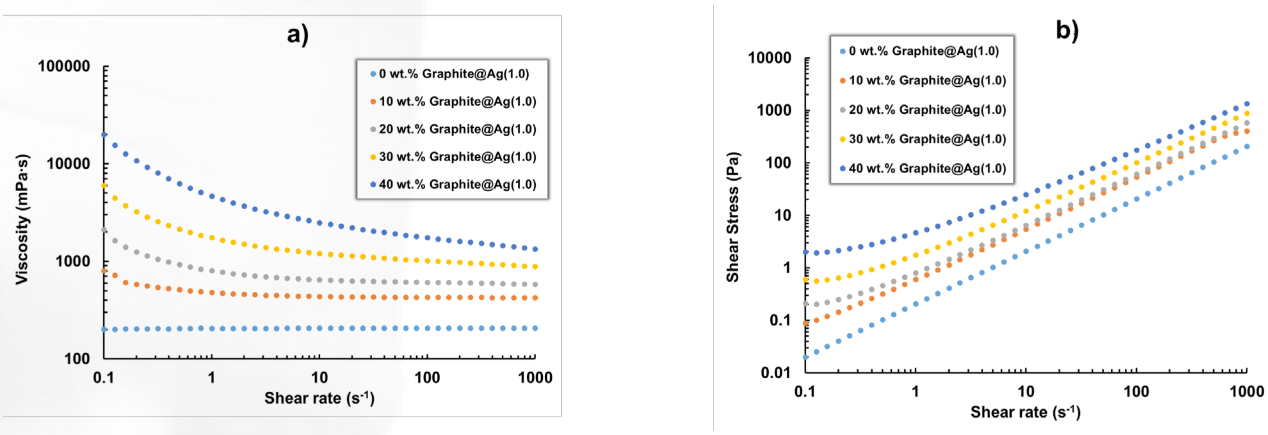


**Figure 4:** *The dependence of viscosity and shear stress on shear rate.*

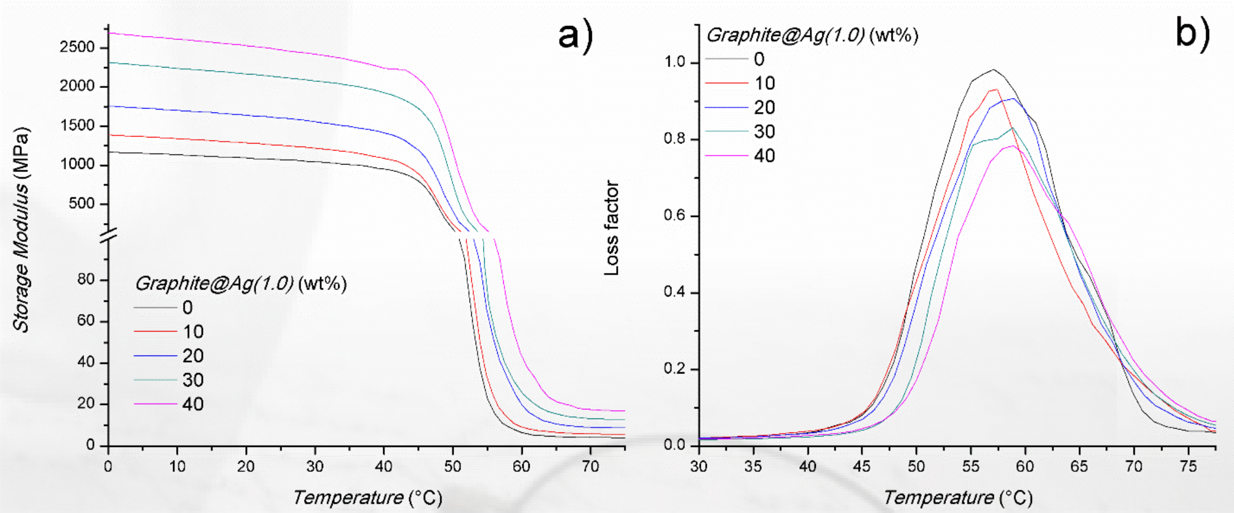


**Figure 5:** *The dependence of storage modulus (a) and loss factor (b) on temperature for different mass fractions of Graphite@Ag(1.0) particles in the suspension.*

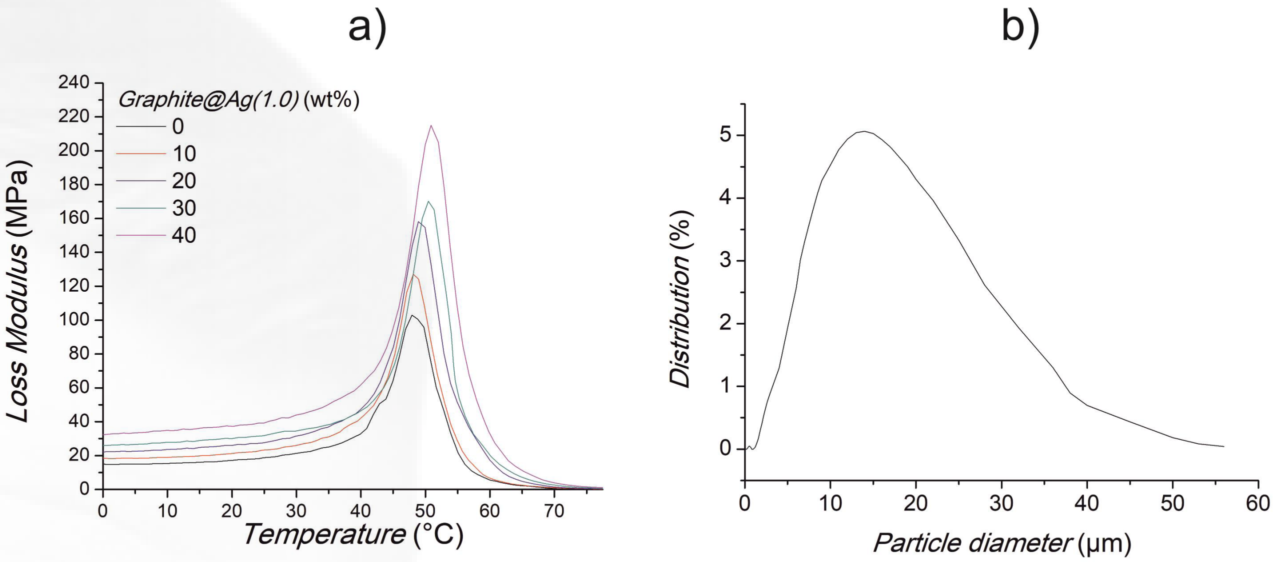


**Figure 6:** *The loss modulus of epoxy composites with different mass fractions of Graphite@Ag(1.0) particles (a), and size distribution of Graphite@Ag(1.0) particles (b)*

According to Figure 4, it can be concluded that, with an increase in the concentration of modified graphite particles, the viscosity of the suspension also increases. At 25°C the epoxy resin without Graphite@Ag(1.0) behaves essentially Newtonian, with viscosity nearly constant (207 mPa·s) over 0.1–1000 $s^{-1}$ (Figure 4. a). Incorporating Graphite@Ag(1.0) particles increases the low-shear viscosity by orders of magnitude and induces pronounced shear-thinning. At 0.1 $s^{-1}$ viscosity rises from 207 mPa·s for the pure epoxy resin to 20058 mPa·s for the 40 wt.% of Graphite@Ag(1.0), while at 1000 $s^{-1}$ it is 201 mPa·s (0 wt.%) and 1341 mPa·s (40 wt.%). From Table 1 it can be concluded that the shear-thinning factor ($\eta_{0.1}/\eta_{1000}$) increases progressively with increasing graphite content. This indicates an increasingly pronounced dependence of viscosity on shear rate. A higher particle loading offers greater resistance to flow at low shear rates, but as the shear rate increases, the viscosity decreases substantially. The corresponding flow curves (Figure 4. b) are well described by the Ostwald–de Waele law, with the flow index n decreasing systematically with filler content (Table 1.). These trends reflect sub-linear growth of stress with shear rate as the suspension becomes increasingly non-Newtonian. Therefore, no clear yield stress is evident within the 0.1–1000 $s^{-1}$ shear rate.

**Table 1:** *Influence of graphite@Ag content on low- and high-shear viscosity and the flow index n (25 °C)*

| Graphite@Ag [wt.%] | η (0.1 $s^{-1}$) [mPa·s] | η (1000 $s^{-1}$) [mPa·s] | η(0.1)/η(1000) | n |
|---|---|---|---|---|
| 0 | 207.2 | 201.3 | 1.0 | 1.00 |
| 10 | 890.0 | 423.3 | 2.1 | 0.96 |
| 20 | 2121.3 | 579.8 | 3.7 | 0.91 |
| 30 | 6008.3 | 883.9 | 6.8 | 0.84 |
| 40 | 20058.0 | 1340.8 | 15.0 | 0.75 |

A higher particle mass fraction, together with the platelet-like graphite morphology, promotes the formation of additional particle-particle and particle–polymer interactions (van der Waals and electrostatic), thereby increasing the resistance to flow at low shear rates (Naz et al., 2016). Moreover, higher particle loadings increase interfacial contact area, owing to the graphite's non-spherical (platelet) morphology. With increasing shear, this weakly bonded network is progressively disrupted, and the platelets tend to align with the flow, leading to the observed pseudoplasticity (shear-thinning) and to the convergence of apparent viscosity values at high shear rates. In practice, formulations with ≥30 wt.% demand higher shear rates (or modest heating) for mixing and vacuum degassing.

Viscosity plays a critical role in the manufacturing of large-surface or complex-shaped epoxy-based composite components for security applications. Excessively high viscosity hinders resin flow, complicating uniform distribution and thorough impregnation of reinforcements. Consequently, precise rheological control and optimization are crucial to ensure high-quality, reliable components.

Empirically, liquid, uncrosslinked epoxy composite systems with a zero-shear viscosity ($\eta_0$) below $4.5 \cdot 10^5$ Pa·s are generally considered pourable and thus suitable for fabrication. Moreover, even modest increases in shear rate during mixing lead to a sharp reduction in apparent viscosity. This behavior facilitates homogenization of the material and supports defect-free consolidation in complex geometries.

DMTA provides a robust framework for probing the viscoelastic response of polymer/composite systems. In this context, the storage modulus G′ quantifies the elastic energy stored and recovered during deformation, whereas the loss modulus G′ reflects the viscous dissipation. Temperature-sweep experiments (Figure 5) show that all specimens follow the same qualitative trend in G′, G′, and tan δ: G′ attains its highest values in the glassy state and decreases as temperature rises, while G′ increases over the low-temperature interval (0–33°C) as segmental mobility grows, culminating in a tan δ maximum that marks the glass-transition region. The ranking of stiffness is governed by graphite content. The 40 wt.% composite exhibits the largest G′, followed by 30, 20, and 10 wt.% formulations, with the neat epoxy lowest. In the 0–44°C interval, the G′ decreases for all specimens, with a more pronounced drop at higher graphite contents; the characteristic slopes are 13.1, 12.4, 11.2, 9.1, and 7.0 MPa/°C for 40, 30, 20, 10 wt.% and the neat resin, respectively.

The glass transition ($T_g$) shifts to higher temperature with increasing graphite loading: for the neat matrix the transition is essentially traversed above 61°C, whereas for the 40 wt.% composite it occurs above 66°C. This shift reflects restricted cooperative motions of the polymer segments caused by graphite platelets and their interfacial interactions with the matrix (including hydrogen bonding), which stabilize the structure and delay relaxation to higher temperatures (De La Fuente et al., 2003). Consequently, substantial compliance (rubbery response) is achieved only at elevated temperatures. Notably, the stiffness ranking observed in the glassy state persists into the rubbery region as well (Figure 6).

DMTA temperature sweeps show a slight, monotonic upshift of the $T_g$ with increasing Graphite@Ag(1.0) content: 57.1, 57.5, 58.1, 59.0, and 59.9°C for 0, 10, 20, 30, and 40 wt.%, respectively. This indicates modest restriction of cooperative segmental motions by the platelet filler and interfacial constraints. Consistently, the damping peak (tan δ max) decreases with loading: 0.98, 0.93, 0.89, 0.82, and 0.76 for 0–40 wt.%. This reflects reduced viscous dissipation and a larger elastic contribution (lower G”/G′). Outside the transition region, the moduli trends confirm rheological stability with low energy loss across the examined range, supporting the suitability of all formulations for service under ambient conditions. A brief comparison of the results of this study and some previous studies is shown in Table 2.

**Table 2:** *Comparison of DMTA results for epoxy-based composites with graphite or carbon reinforcement*

| Study | Epoxy resin system | Reinforcement / Filler | $T_g$ range (°C) | Max modulus (MPa) | Notes |
|---|---|---|---|---|---|
| **This study** | Epoxy casting resin (type W300) + amine hardener | Modified graphite particles (0–40 wt.%) | 57.1–59.9 (from peak tanδ) | G' = 2692.4 MPa at 0 °C (40 wt.%) | Graphite improves stiffness and $T_g$; viscosity limits casting above 30 wt.% |
| **(Sudar-shanRao, 2021)** | LAPOX-12 epoxy + polyamine K5 hardener | Carbon fabric + graphite (0–6 wt.%) | 118.1–133.0 (from E″ and tanδ peaks) | E'=28.18 GPa at RT (6 wt.%) | Significant increase in modulus and damping with graphite loading |
| **(Stark et al., 2015)** | Hexcel 6376C epoxy prepreg | Unidirectional carbon fibers | 139.4–223.8 (E″ peak, extrapolated to 0.01 Hz) | Not reported | $T_g$ strongly dependent on curing degree; DMA used to monitor curing progress |

The DMTA results obtained in this study were compared with those reported in previous literature. As shown in Table 1, although the absolute values of $T_g$ and storage modulus vary depending on the epoxy system and filler type, a consistent trend is observed—graphite or carbon reinforcement increases both stiffness and $T_g$. In particular, the present work demonstrates that graphite contents above 30 wt.% lead to significant increases in viscosity, which may limit their application in casting processes without using vacuum and vibrations. This aspect is not covered in the compared studies and highlights the importance of rheological characterization alongside mechanical performance evaluation.

### *The Electrical Resistivity and EMI Shielding Effectiveness*

One of the most important physical properties that influence the behavior of materials in the EMI SE process is electrical resistance. This parameter can significantly help in the selection of materials for making composites intended to achieve electromagnetic compatibility. Measurements of electrical resistance of particles of commercial graphite and graphite modified with silver deposits in the presented study show the following results: for the particles of untreated graphite, Graphite@Ag(0.5), Graphite@Ag(1.0), and Graphite@Ag(1.5) the following values of resistivity were 0.91 mΩ, 0.39 mΩ, 0.11 mΩ, and an impressive 0.07 mΩ, respectively. These resistance test results clearly show that as the mass of silver deposition decreases, the electrical resistivity of particles that contribute to EMI SE and signal beam attenuation increases. This substantial enhancement emphasizes the effectiveness of silver modification in boosting conductivity, representing a significant advancement in material performance, which confirms the enhanced EMI SE characteristics, especially wave reflection.

The study focused on the potential application of composite materials for EMI SE within the X-band frequency range (8.2–12.4 GHz). Figure 7 displays the overall EMI SE of samples with different silver-to-graphite ratios (Figure 7a) and varying mass fractions of Graphite@Ag(1.0) embedded in an epoxy matrix (Figure 7b).

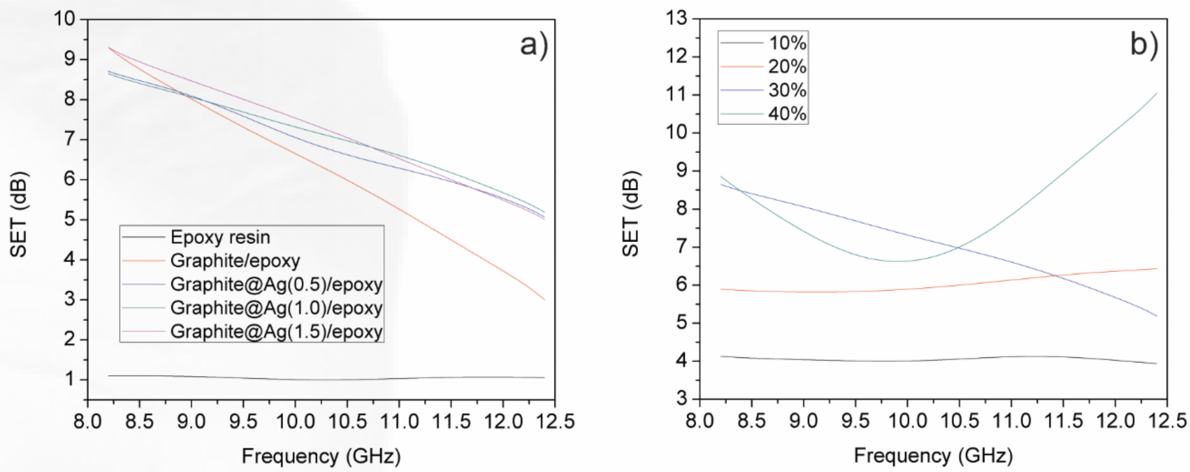


**Figure 7:** *Measured EMI effectiveness shielding of samples with varying silver-to-graphite ratios (a), and different mass fractions of Graphite@Ag(1.0) within the epoxy matrix (b) in X-band frequency range.*

The data on the EMI shielding coefficients reveal that increasing the silver content on the graphite surface correlates with higher shielding performance. Analysis of the results in Figure 7a and the accompanying supplementary material shows the total EMI SE for various epoxy resin composites: 30% Graphite/epoxy, 30% Graphite@Ag(0.5)/epoxy, 30% Graphite@Ag(1.0)/epoxy, and 30% Graphite@Ag(1.5)/epoxy, which yield average SE values of 6.02, 6.91, 7.06, and 7.21 dB, respectively. This trend indicates that increasing silver loading on the graphite surface can boost shielding efficiency by approximately 21%. Similar findings were reported by Stupar et al. (Stupar et al., 2022), where depositing silver onto carbon fabric enhanced both electrical conductivity and EMI shielding capabilities. Further analysis of the reflection and absorption characteristics within the X-band shows that reflection increases from 4.49 dB for pure graphite to 6.01 dB for Graphite@Ag(1.5)/epoxy, while absorption decreases from 1.72 dB to 1.18 dB. This behavior is likely due to the high electrical conductivity of silver, which promotes electromagnetic wave scattering within the composite, thereby contributing to SE. Examining the influence of particle content, the data on samples with 30% Graphite@Ag(1.0) indicate that increasing the particle mass fraction from 10% to 40% enhances shielding performance, with wave attenuation values of 3.68, 6.04, 7.06, and 8.01 dB, respectively. This is due to the higher particle concentrations leading to more frequent interactions and scattering of electromagnetic waves, weakening the wave strength. Similar observations were made by Wei et al. (Wei et al., 2021), pointing out that as the concentration of active expanded graphite particles in the polymer matrix increased, the same effect was noted. Notably, the sample containing 40% graphite@Ag(1.0) in epoxy resin exhibited a distinct EMI SE trend, which is attributed to the formation of larger agglomerates during manufacturing. These agglomerates disturb the uniform particle distribution, resulting in a more porous structure that enhances multiple scattering of electromagnetic waves and thus improves the overall shielding performance. By comparing the results from the literature and the results of the test of the effectiveness of weakening the strength of the wave beam, the lower efficiency of the tested can be explained by the thickness of the composite material. By increasing the material or forming a honeycomb contour of the material, it is possible to increase the efficiency of the material. Therefore, by modifying this composite, it is possible to improve its EMI SE. Also, by further crushing the particles, it is possible to improve the packing of the particles in the composite, which would reduce the possibility of beam leakage in the space between the particles. Table 2 summarizes these findings alongside relevant data from other studies. Table 3 shows the results presented in this paper and those of other studies.

**Table 3:** *Electrical conductivity and average EMI SE for different composites.*

| Composite | Filler content | Sample thickness, (mm) | SET, (dB) | Frequency, (GHz) | Ref. |
|---|---|---|---|---|---|
| **Carbon black/EPDM** | 50% | 5.5 | ~8 | 8.2-12.4 | (Ghosh & Chakrabarti, 2000) |
| **Aramid nanofiber assisted preparation of 3D-oriented graphite/silicone composite slices** | 32.68% | 2 | 20.15 | 8.2-12.4 | (Lei et al., 2023) |
| **Graphite nanoparticles/PE** | 10 % | 1 | ~22 | 26-37.5 | (Vovchenko et al., 2018) |
| **Carbon nanotubes/PE** | 4.5 | 1 | 42 | 26-37.5 | (SudarshanRao, 2021) |
| **graphite/PVDF** | 10% | / | 2.25 | 8.2-12.4 | (Kumaran et al., 2015) |
| **1 wt. % of AgNP-10 wt. % graphite/PVDF** | / | / | 4.9 | 8.2-12.4 | (SudarshanRao, 2021) |
| **e Ag-EG (10 wt.%) @pPDMS** | / | 2 | 12 | 8.2-12.4 | (Lin et al., 2025) |
| **Graphite/epoxy** | 7 | 2 | 19-21 | 8.2-12.4 | (Gümüş et al., 2023) |
| **Carbon black/epoxy** | 7 | 2 | 9 | 8.2-12.4 | (Gümüş et al., 2023) |
| **Graphite@Ag(1.5)/epoxy** | 30 % | 1 | 7.21 | 8.2-12.4 | **this study** |
| **Graphite@Ag(1.0)/epoxy** | 40 % | 1 | 8.01 | 8.2-12.4 | **this study** |

## CONCLUSION

This study focuses on the modification of graphite particles using varying amounts of synthesized silver conductive dispersion and their application in the production of composite materials with an epoxy matrix. Additionally, it explores potential applications in EMI SE and material strengthening. The results obtained from the study are as follows:

- The scanning electron microscopy analysis indicates that the appearance of silver agglomerates is significantly influenced by the amount of electroconductive dispersion used. The increase of dispersion amount increases the agglomeration of silver particles.
- The analysis of the elemental composition of the particles confirms that, as the volume of the electroconductive complex used during the modification process increases, the amount of elemental silver deposited on the surface of the graphite particles also increases.
- The rheological characterization shows that increasing the concentration of modified graphite (Graphite@Ag(1.0)) raises the suspension viscosity while remaining within a practical processing window. The storage modulus G′ attains its highest values in the glassy regime and decreases with further temperature increase. In addition, higher Graphite@Ag(1.0) loadings shift the glass

transition to higher temperatures; at 40 wt%, the $T_g$ rises by nearly 3°C, indicating only a modest effect on the breadth of the glass-transition region. Since all $T_g$ values exceed 50°C – and silver further elevates $T_g$ – the formulations operate below $T_g$ within the intended service window (<50°C), which is beneficial for dimensional stability, homogenized stress transfer, and retention of modulus in use. The deposition of silver particles onto the graphite surface significantly increases the electrical conductivity, which highly contributes to EMI SE increasing.
- The measured values of coefficients and the effectiveness of EMI SE in composites show that, as the mass fraction of silver on the graphite surface increases, the EMI SE also rises. Total EMI SE for various epoxy resin samples: 30%Graphite/epoxy, 30%Graphite@Ag(0.5)/epoxy, 30% Graphite@Ag(1.0)/epoxy, 30% Graphite@Ag(1.5)/epoxy yield average values of 6.02, 6.91, 7.06, and 7.21 dB, respectively, in the X-band. Also, the increase of the overall number of particles subsequently increases EMI SE properties.
- In summary, this cost-effective modification method enhances the properties of graphite, which are essential for applications in composite production and EMI shielding materials. Additionally, incorporating modified graphite particles improves the overall properties of the composite. Therefore, graphite particles modified with elemental silver can fulfill the stringent requirements for producing composites that are subjected to mechanical stress while also minimizing EMI.

## ACKNOWLEDGEMENT

This work was financially supported by the Ministry of Science, Technological Development, and Innovation of the Republic of Serbia (Contract No. 451-03-137/2025-03/200115).

## REFERENCES

Behera, B. K., Parveen, J. S., Manohar, M., Begum, S., & Thirumurugan, M. (2024). The Influence of Graphite Filler on the Viscoelastic and Mechanical Characteristics of PC/ABS Hybrid Composite for Automotive Applications. *Journal of Mechanical Engineering*, *21*(1), 143–161. https://doi.org/10.24191/jmeche.v21i1.25364

Bhardwaj, P., & Nirmala, A. (2020). Antistatic and microwave shielding performance of polythiophene-graphene grafted 3-dimensional carbon fibre composite. *Diamond & Related Materials*, *106*, 107871. https://doi.org/10.1016/j.diamond.2020.107871

Cheng, Z., Wang, R., Wang, Y., Cao, Y., Shen, Y., Huang, Y., & Chen, Y. (2023). Recent advances in graphene aerogels as absorption-dominated electromagnetic interference shielding materials. *Carbon*, *205*, 112–137. https://doi.org/10.1016/j.carbon.2023.01.032

De La Fuente, J. L., Fernández-García, M., & Cerrada, M. L. (2003). Viscoelastic behavior in a hydroxyl-terminated polybutadiene gum and its highly filled composites: Effect of the type of filler on the relaxation processes. *Journal of Applied Polymer Science*, *88*(7), 1705–1712. https://doi.org/10.1002/app.11941

Fu, D., Yang, R., Wang, Y., Wang, R., & Hua, F. (2022). Silver Nanowire Synthesis and Applications in Composites: Progress and Prospects. *Advanced Materials Technologies*, *7*(11), 2200027. https://doi.org/10.1002/admt.202200027

Gahlout, P., & Choudhary, V. (2019). Microwave shielding behaviour of polypyrrole impregnated fabrics. *Composites Part B*, *175*, 107093. https://doi.org/10.1016/j.compositesb.2019.107093

Ghosh, P., & Chakrabarti, A. (2000). Conducting carbon black filled EVA vulcanizates: Assessment of dependence of physical and mechanical properties and conducting character on variation of filler loading. *Journal of Polymer Materials*, *17*(3), 291–304. https://doi.org/10.1016/S0014-3057(99)00157-3

Greety DJ, B., & Wessley, G. J. J. (2024). A study on EMI shielding in aircraft: introduction, methods and significance of using electrospun nanocomposites. *Journal of Space Safety Engineering*, *11*(1), 150–160. https://doi.org/10.1016/j.jsse.2024.01.001

Gümüş, E., Yağımlı, M., & Arca, E. (2023). Investigation of the Dielectric Properties of Graphite and Carbon Black-Filled Composites as Electromagnetic Interference Shielding Coatings. *Applied Sciences*, *13*(15), 8893. https://doi.org/10.3390/app13158893

Hamamah, F., Ahmad, W. F. H. W., Gomes, C., Isa, M. M., & Homam, M. J. (2019). Concerns on the Risk of Malaysian Civil and Defense Systems Due to Intentional Electromagnetic Interference. *APACE 2019 – 2019 IEEE Asia-Pacific Conference on Applied Electromagnetics, Proceedings*, 25-27 *November 2019*, 1–6. https://doi.org/10.1109/APACE47377.2019.9021096

Hong, X., Gao, Y., Ji, M., Li, J., Ding, L., Yu, Z., & Chang, K. (2024). Highly valent cobalt-manganese spinel nanowires induced by fluorine-doping for durable acid oxygen evolution reaction. *Journal of Alloys and Compounds*, *1007*, 176500. https://doi.org/10.1016/j.jallcom.2024.176500

Hu, J., Xu, X., Cao, D., & Liu, G. (2019). Analysis and optimization of electromagnetic compatibility for electric vehicles. *IEEE Electromagnetic Compatibility Magazine*, *8*(4), 50–55. https://doi.org/10.1109/MEMC.2019.8985599

Hwan, S., Yu, S., Shahzad, F., Hong, J., Jin, S., Nyon, W., Man, S., & Min, C. (2019). Low percolation 3D Cu and Ag shell network composites for EMI shielding and thermal conduction. *Composites Science and Technology*, *182*, 107778. https://doi.org/10.1016/j.compscitech.2019.107778

Iqbal, S., Shah, J., Kotnala, R. K., & Ahmad, S. (2019). Highly efficient low cost EMI shielding by barium ferrite encapsulated polythiophene nanocomposite. *Journal of Alloys and Compounds*, *779*, 487–496. https://doi.org/10.1016/j.jallcom.2018.11.307

Kumaran, R., Alagar, M., Dinesh Kumar, S., Subramanian, V., & Dinakaran, K. (2015). Ag induced electromagnetic interference shielding of Ag-graphite/PVDF flexible nanocomposites thinfilms. *Applied Physics Letters*, *107*(11), 113107. https://doi.org/10.1063/1.4931125

Lei, Z., Zhu, K., Lv, F., Hu, M., Liu, X., Wei, J., Lyu, S. S., Mo, D. chuan, & Hu, Y. (2023). Aramid nanofiber assisted preparation of 3D-oriented graphite/silicone composite slices with high through-plane thermal conductivity and efficient electromagnetic interference shielding. *Composites Science and Technology*, *243*, 110246. https://doi.org/10.1016/j.compscitech.2023.110246

Lin, D., Yu, C., Guo, J., Li, G., Jiang, X., Yao, Y., & Zhang, X. (2025). Polyethylene glycol modified polysiloxane and silver decorated expanded graphite composites with high thermal conductivity, EMI shielding, and leakage-free performance. *Composites Part B: Engineering*, *291, 112041*. https://doi.org/10.1016/j.compositesb.2024.112041

Liu, Q., & Xu, B. (2020). Solution Evaporation-Driven Crumpling and Assembling of Large-Accessible Space, High-Mechanical Strength Graphene/Carbon Nanotubes Composite Nanoparticles. *ACS Applied Materials & Interfaces*, *12*, 43058–43064. https://doi.org/10.1021/acsami.0c10532

Naz, A., Kausar, A., & Siddiq, M. (2016). Influence of Graphite Filler on Physicochemical Characteristics of Polymer/Graphite Composites: A Review. *Polymer - Plastics Technology and Engineering*, *55*(6), 604–625. https://doi.org/10.1080/03602559.2015.1098697

Singh A.P., Mishra M., Sambyal P., Gupta B.K., Singh B.P., Chandra A., Dhawan S.K. (2014). Encapsulation of γ-Fe2O3 decorated reduced graphene oxide in polyaniline core-shell tubes as an exceptional tracker for electromagnetic environmental pollution. *Journal of Materials Chemistry A, 2,* 3581–3593. https://doi.org/10.1039/c3ta14212d

Stark, W., Jaunich, M., & McHugh, J. (2015). Dynamic Mechanical Analysis (DMA) of epoxy carbon-fibre prepregs partially cured in a discontinued autoclave analogue process. *Polymer Testing*, *41*, 140–148. https://doi.org/10.1016/j.polymertesting.2014.11.004

Stupar, S. L., Vuksanović, M. M., Mijin, D., Bučko, M. M., Joksimović, V. J., Barudžija, T. S., & Tanić, M. N. (2023). Functional nano-silver decorated textiles for wearable electronics and electromagnetic interference shielding. *Materials Today Communications*, *34,* 105312. https://doi.org/10.1016/j.mtcomm.2023.105312

Stupar, S. L., Vuksanović, M. M., Mijin, D., Milanović, B. C., Joksimović, V. J., Barudžija, T. S., & Knežević, M. R. (2022). Multispectral electromagnetic shielding and mechanical properties of carbon fabrics reinforced by silver deposition. *Materials Chemistry and Physics*, *289,* 126495 . https://doi.org/10.1016/j.matchemphys.2022.126495

Stupar, S. L., Wang, Y., Wang, J., Timotijević, M., Mijin, D., Rakočević, L., Milović, M., & Vučković, N. (2025). Effects of silver coated graphite particles on mechanical and electromagnetic shielding properties of an epoxy resin. *Surfaces and Interfaces*, *68,* 106663. https://doi.org/10.1016/j.surfin.2025.106663

SudarshanRao, K. (2021). Dynamic mechanical behavior of unfilled and graphite filled carbon epoxy composites. *IOP Conference Series: Materials Science and Engineering*, *1126*(1), 012033. https://doi.org/10.1088/1757-899x/1126/1/012033

Uma Varun, V., Rajesh Kumar, B., & Etika, K. C. (2019). Hybrid polymer nanocomposites as EMI shielding materials in the X-band. *Materials Today: Proceedings*, *28*, 796–798. https://doi.org/10.1016/j.matpr.2019.12.300

Vovchenko, L., Matzui, L., Oliynyk, V., Launets, V., Mamunya, Y., & Maruzhenko, O. (2018). Nanocarbon/polyethylene composites with segregated conductive network for electromagnetic interference shielding. *Molecular Crystals and Liquid Crystals*, *672*(1), 186–198. https://doi.org/10.1080/15421406.2018.1555349

Vučković, N., Glođović, N., Radovanović, Ž., Janaćković, Đ., & Milašinović, N. (2021). A novel chitosan/tripolyphosphate/L-lysine conjugates for latent fingerprints detection and enhancement. *Journal of Forensic Sciences*, *66*(1), 149–160. https://doi.org/10.1111/1556-4029.14569

Wang, Y., Peng, H. K., Li, T. T., Shiu, B. C., Zhang, X., Lou, C. W., & Lin, J. H. (2020). Layer-by-layer assembly of low-temperature in-situ polymerized pyrrole coated nanofiber membrane for high-efficiency electromagnetic interference shielding. *Progress in Organic Coatings*, *147*, 105861. https://doi.org/10.1016/j.porgcoat.2020.105861

Wei, B., zhang, L., & Yang, S. (2021). Polymer composites with expanded graphite network with superior thermal conductivity and electromagnetic interference shielding performance. *Chemical Engineering Journal*, *404*, 126437. https://doi.org/10.1016/j.cej.2020.126437

Wiśnios, M., Mazur, M., Paś, J., Łukasiak, J. M., Gladys, S., Wetoszka, P., & Białek, K. (2025). Operation of Electronic Security Systems in an Environment Exposed to Conducted and Radiated Electromagnetic Interference. *Electronics (Switzerland)*, *14*(14), 1–33. https://doi.org/10.3390/electronics14142851

Yan, Y., & Cao, W. (2021). The mining method of anti-electromagnetic interference for electronic equipment in coal mine by considering network communication technology. *Microelectronics Journal*, *109*, 104987. https://doi.org/10.1016/j.mejo.2020.104987

Yu-ichi Hayashi. (2016). State-of-the-art research on electromagnetic information security. *Radio Science*, *51*, 1213–1219. https://doi.org/doi:10.1002/2016RS006034

Zhang, J., Li, X., Zhang, M., Zhu, Q., & Sun, X. (2022). Flexible and ultra-thin silver films with superior electromagnetic interference shielding performance: Via spin-coating silver metal-organic decomposition inks. *Materials Advances*, *3*(1), 647–657. https://doi.org/10.1039/d1ma00918d

Zhang, Y. Z., Wang, Y., Jiang, Q., El-Demellawi, J. K., Kim, H., & Alshareef, H. N. (2020). MXene Printing and Patterned Coating for Device Applications. *Advanced Materials*, *32*(21), 1908486. https://doi.org/10.1002/adma.201908486

Zheng, X., Zhang, H., Liu, Z., Jiang, R., & Zhou, X. (2022). Functional composite electromagnetic shielding materials for aerospace, electronics and wearable fields. *Materials Today Communications*, *33*, 104498. https://doi.org/10.1016/j.mtcomm.2022.104498